The antitumoral activity of TLR7 ligands is corrupted by the microenvironment of pancreatic tumors

Marie Rouanet, Naima Hanoun, Cindy Ferreira, Pierre Garcin, Martin Sramek, Godefroy Jacquemin, Agnès Coste, Delphine Pagan, Carine Valle, Emeline Sarot, et al.

Version of Record: https://www.sciencedirect.com/science/article/pii/S1525001622000181
Manuscript_b2c685171eb40dbb33d2e2b16e4691af

The antitumoral activity of TLR7 ligands is corrupted by the microenvironment of pancreatic tumors

Marie Rouanet[1,2], Naima Hanoun1, Hubert Lulka[1], Cindy Ferreira[1], Pierre Garcin[1], Martin Sramek[1], Godefroy Jacquemin[4], Agnès Coste[4], Delphine Pagan[1], Carine Valle[3], Emeline Sarot[3], Vera Pancaldi[1], Frédéric Lopez[3], Louis Buscail[1,2] and Pierre Cordelier[1] *.

1: Université Fédérale Toulouse Midi-Pyrénées, Université Toulouse III, Paul Sabatier, INSERM, CRCT, Toulouse, France.

2: Department of Gastroenterology and University of Toulouse III, Rangueil Hospital, Toulouse, France.

3: Technological cluster, INSERM, CRCT, Toulouse, France.

4: Université Fédérale Toulouse Midi-Pyrénées, Université Toulouse III, Paul Sabatier, INSERM, CNRS, EFS, RESTORE, Toulouse, France.

*: corresponding author.

Pierre Cordelier, Cancer Research Centre of Toulouse (CRCT),

INSERM U1037, 2, avenue Hubert Curien, 31100 Toulouse, France.

Email: pierre.cordelier@inserm.fr

Keywords: pancreatic cancer, toll like receptors, tumor microenvironment

Short title: TLR7 dual effect on pancreatic tumors

Abstract

Toll like receptors (TLR) are key players in the innate immune system. Recent studies have suggested that they may impact the growth of pancreatic cancer, a disease with no cure. Among them, Toll like receptor-7 (TLR7) shows promise for therapy but may also promotes tumor growth. Thus, we aimed to clarify the therapeutic potential of TLR7 ligands in experimental pancreatic cancer models, to open the door for clinical applications. *In vitro*, we found that TLR7 ligands strongly inhibit the proliferation of both human and murine pancreatic cancer cells, as compared to Toll like receptor-2 agonists. Hence, TLR7 treatment alters cancer cells cell cycle and induce cell death by apoptosis. *In vivo*, TLR7 agonist therapy significantly delays the growth of murine pancreatic tumors engrafted in immunodeficient mice. Remarkably, TLR7 ligands administration instead increases tumor growth and accelerates animal death when tumors are engrafted in immunocompetent models. Further investigations revealed that TLR7 agonists modulate the intratumoral content and phenotype of macrophages, and that depleting such tumor-associated macrophages strongly hampers TLR7 agonists-induced tumor growth. Collectively, our findings shine a light on the duality of action of TLR7 agonists in experimental cancer models and calls into question their use for pancreatic cancer therapy.

Introduction

Pancreatic adenocarcinoma (PDAC) is a disease with no cure projected to become the second deadliest cancer worldwide by 2025[1], with 5-year survival at less than 10%[2]. PDAC's dismal prognosis is due to late diagnosis and to the lack of effective therapies[3]. Thus, there is an urgent need to define successful treatments to improve the prospects of patients diagnosed with PDAC.

Toll like receptors (TLRs) are pattern recognition receptors that are expressed on innate immune cells and in tumors[4], including PDAC[5]. TLR ligands include bacterial and viral motifs (PAMPs for pathogen-associated molecular patterns), and damage-associated molecular patterns (DAMPs)[6]. TLRs recently emerged as promising targets, as they demonstrate therapeutic interest both on cancer cells and other cells in the tumor microenvironment (TME). Indeed, TLR activation can result in lethal autophagy, cell death by apoptosis or pyroptosis of cancer cells[7]. In addition, TLRs control tumor-promoting inflammatory signaling pathways common to both myeloid and lymphoid cells. Consequently, TLR manipulation has an impact not only on myeloid cells, but it also increases the activity, specificity and efficacy of adaptive immunity within the TME[7]. Recently, TLR2 agonists mimicking microbial signals were found to generate tumor-suppressive macrophages[8]. In another example, stimulating TLR7, an endosomal single strand (ss) RNA receptor associated with viral response and proinflammatory cytokines and type I interferon production[9], inhibits programmed cell death protein 1 (PD-1) expression on T cells and promotes CD8- T-cell cytotoxic responses[10]. TLR7 agonists include benzapines and imidazolquinolines, with FDA-approved imiquimod and its more active version resiquimod (R848). Such small-molecule agonists demonstrated preliminary antitumoral efficacy but require further optimization to reach their full therapeutic potential[11].

This is particularly true for PDAC, as TLR7 engagement demonstrates diametrically opposite effects on cancer cell lines and tumor outcome[12]. *In vitro*, TLR7 ligation results in both inhibition[13] and stimulation of cancer cell proliferation[14]. *In vivo*, TLR7 promotes pancreatic carcinogenesis in mice by driving stromal inflammation[15] and participates in microbiome-induced tumor promotion[5]. On the other hand, in interventional studies, TLR7 (adjuvant) therapy is often associated with beneficial immune antitumor response[16–18]. For instance, stromal rather than neoplastic TLR7 remodels tumor and host response to increase survival of mice with experimental PDAC, notably after improving cancer-associated cachexia[18]. On the contrary, Calore *et al.* recently demonstrated that TLR7 may also actively participate in cachexia, strongly arguing that interfering with TLR7 may serve as a potential therapy for the treatment of this highly debilitating syndrome associated to cancer[19]. Collectively, although TLR7 is expressed in cancer lesions[5], mainly within the tumor stroma[18], studies in well-defined experimental models are lacking to definitely address the therapeutic interest of TLR7 activation in PDAC management.

In this study, we investigated whether novel TLR agonists[20] elicit anti-proliferative and anti-tumoral responses in immunodeficient or syngeneic orthotopic PDAC models. Remarkably, these models were generated with the same primary cell line, to determine TLR7 intrinsic action on neoplastic cells, but also on experimental tumors in the presence or not of a functional immune TME. We first demonstrate that *in vitro*, TLR7 agonists potently inhibit human and murine PDAC cell lines proliferation and induce cancer cell death by apoptosis. When tumors are engrafted in immunodeficient animals, TLR7 treatment translates into a significant delay in inhibition of experimental tumor progression and increase in mice survival. On the contrary, treating orthotopic PDAC tumors established in fully immunocompetent animals with TLR7 agonists results in

tumor promotion and decrease in mice survival. We found that TLR7 agonists alter the content and the phenotype of tumor macrophages, and that depleting macrophages blunts the protumoral activity of TLR ligands. Collectively, our data demonstrate that TLR7 agonists have can be of interest to target PDAC cancer cells, but they also induce a tumor promoting TME, which strongly makes us question their potential as a therapy for patients with PDAC.

Results

TLR7 agonists inhibit PDAC cancer cells proliferation and induce cell death by apoptosis.

For this study, we selected murine R211 cells derived from genetically engineered mouse models of PDAC with *KRAS* activating mutation and loss in *TP53*[21]. These cells are closely resembling tumor genetic and phenotypic landscapes and recapitulate tumor architecture and growth when implanted in mice pancreas. We found that human and mice pancreatic cancer cells express detectable levels of TLR2 and TLR7, with R211 expressing the highest levels of the candidate TLRs (Supplemental Figure 2A). We generated R211 cells expressing a nuclear, green fluorescent protein (R211-NucG) to allow for non-invasive, longitudinal analysis of cell proliferation using the Incucyte Zoom. R211-NucG cells were treated with a panel of novel TLR2 and TLR7 agonists[20]. As controls, cells were left untreated, or treated with SSRNA40 with the cationic lipid LyoVec to protect from degradation and facilitate uptake (TLR7/8 agonist), and PAM3CSK4 (TLR2/1 agonist). Table 1 and Supplemental Figure 2 shows that TLR7 agonists CL264 and ssRNA-40 moderately inhibit PDAC cell proliferation (Supplemental Figure 2B-C). On the contrary, PAM3CSK4 (TLR2/1 agonist, Supplemental Figure 2D), CL307 and CL347 (TLR7 agonists coupled with spermine and conjugated with a

bis(phytanyl) phosphonate group, respectively, Supplemental Figure 2E and Figure 1A), CL419 (TLR2 agonist coupled with spermine and conjugated with a bis(phytanyl) phosphonate group, Supplemental Figure 2F) and CL553 (TLR2/7 agonist coupled with spermine and conjugated with a bis(phytanyl) phosphonate group, Supplemental Figure 2G) impair PDAC cell lines cell proliferation. However, CL347 demonstrates the strongest antiproliferative and proapoptotic activity (IC_{50}=77µM±1.2µM, Table 1 and Figure 1A). We confirmed CL347 antiproliferative effect by endpoint cell counting experiments in Mia PACA-2 (human PDAC), PKP16 (murine PDAC) and DT6606 (murine PDAC) cell lines (Supplemental Figure 2I).

We next addressed the specificity of action of CL347 in murine pancreatic cancer cells. Thus, R211 cells were transfected with plasmids expressing hairpins targeting murine TLR7 (mTLR7), as described in Materials and Methods. Control cells were transfected with plasmids expressing random hairpins. As shown in Supplemental Figure 2H, siRNA targeting mTLR7 successfully decreased mTLR7 expression inR211 cells (-61%±10%, $p<0.001$). As expected, control R211 cell proliferation was significantly inhibited following CL347 treatment (Figure 1C). Remarkably, small hairpins RNA targeting mTLR7 significantly protect from CL347 effect, demonstrating that CL347 signals through TLR7 to exert its antiproliferative and cell death induction effect on cancer cells (Figure 1C). We next explored the molecular mechanisms involved in CL347-induced inhibition of cell proliferation. As shown in Figure 1D and Supplemental Figure 2I, CL347 treatment significantly alters the cell cycle distribution of cancer cells, with concomitant increase in cells in S-phase and in cells undergoing apoptosis, and decrease in cells in G2 phase (Figure 1D). We next treated R211 cells with the TLR7 agonists CL347, CL307 and R848. Results shown Figure 1E indicate that CL347 strongly decreases the levels of cyclin E1 and of cyclin B1, and the phosphorylation of histone H3 and of cell

division cycle protein 2 (cdc2). In these cells, CL347 increases PARP and Caspase-3 cleavage by 10 and 109-fold respectively, as compared to mock (Figure 1F). Collectively, these results demonstrate that CL347 signals through TLR7 to alter the cell cycle progression and to induce cell death by apoptosis of pancreatic cancer cells.

***In vivo* TLR7 agonist administration inhibits PDAC cell proliferation and tumor progression and increases mice survival in immunodeficient mice.**

The effect of TLR7 agonists on tumor progression is multifaceted, with an impact on both neoplastic cells and the TME. We first addressed the cell intrinsic activity of the TLR7 agonist CL347 on PDAC models, in the absence of the immune microenvironment. NOD scid gamma (NSG) mice were implanted with CL347-responsive R211 cells expressing red-shifted, firefly luciferase (R211-RSLucF). Tumor growth was monitored non-invasively by detecting luciferase bioluminescence using the Ivis Spectrum. Animals with exponentially growing tumors were treated intraperitoneally with CL347 at the indicated doses. By 15 days following treatment, only 20% (1/5) of mice from the placebo group were alive, while 12 out of 14 mice (85%) receiving CL347 survived during the course of the experiment (Figure 2A). Mice treated with all three doses of CL347 show similar tumor weight (Supplemental Figure 3A) and tumor volume (Supplemental Figure 3B). Importantly, mice treated with the highest dose of CL347 (80µg) show significantly lower tumor viability following treatment, as compared to mice receiving 20µg of the TLR7 agonist ($p<0.01$, Figure 2B). Significant concerns exist about TLR agonists toxicity when administered systemically, despite beneficial effects on tumor response. During this study, we yet did not observed mice weight loss following treatment with CL347 (data not shown). We next investigated the molecular mechanisms involved in CL347 antitumoral effect. As shown in Figure 2C and 2D,

immunohistochemistry detection of Ki67 demonstrated that CL347 treatment significantly reduces the number of proliferating cancer cells (288±24 *vs* 120±11, respectively, $p<0.001$). Collectively, these results demonstrate the antiproliferative action of TLR7 agonists *in vivo*, which translates into improved survival in experimental immunodeficient models of PDAC.

TLR7 treatment favors tumor progression in immunocompetent hosts.

TLR agonists are used against a variety of malignancies to induce antitumoral immunity[7]. We explored whether TLR7 agonist CL347 could activate tolerant host immune system to eradicate experimental PDAC. To this end, R211-RSLucF cells were engrafted in the pancreas of immune competent mice and tumor growth was monitored non-invasively as described before. As expected, host response significantly delayed the increase in tumor burden, suggesting tumor control by immune cancer killing cells (data not shown). To our surprise, we found that TLR7 treatment shortens mice survival, with a dose-dependent trend, when control mice were all alive at the end of the experiment (5/5). In greater details, 40% (2/5) and 60% (3/5) mice with murine pancreatic tumors died following treatment with either 20µg or 40µg, and 80µg of TLR7 agonist (Figure 3A). At the time of killing, mock-treated tumors and tumors receiving TLR7 showed similar weight, volume and viability (Supplemental Figure 3C-E). By immunohistochemistry for Ki67, we found that CL347 treatment leads to tumors with more aggressive phenotypes and higher proliferative index (Figure 3B and 3C). We next treated immunocompetent mice with lower dose of CL347, as TLR7 ligands are well known to exhibit a bell-shape dose response curve when administered *in vivo*. We also injected CL347 intratumorally to ask whether CL347 route of administration may change the therapeutic outcome. Control tumors were injected with PBS (mock) or received I.P.

R848 resiquimod TLR7 agonist. As shown in Figure 3D, mock-treated tumors progressed by 56%±18% during the course of the experiment. With the exception of 3µg of CL347, all tested doses of CL347 significantly increased tumor progression (mean 3.7±0.43-fold increase), regardless of the route of administration. In addition, R848 I.P. injection resulted in similar tumor promotion. Thus, in this model of immune competent pancreatic cancer, CL347 protumoral effect is not bell-shaped, is effective following intratumoral and systemic administration, and can be reproduced by resiquimod.

TLR7 agonists modulate the intratumoral content and phenotype of murine macrophages to promote tumor growth.

Considering the well-described effect of TLR7 on immune cell populations, R211 tumors were analyzed for lymphocytic (CD3) markers. We found that CL347 treatment significantly decreases the number of lymphocytes infiltrating R211 tumors (Figure 4A and 4B); on the other hand, CL347 increases the number of F4/80 positive cells in tumors (Figure 4C and 4D). The F4/80 molecule was established as a unique marker of murine macrophages when a monoclonal antibody was found to recognize an antigen exclusively expressed by these cells. However, recent research has shown that F4/80 is expressed by other immune cells. To get better insights on the nature of F4/80-postive cells within pancreatic tumors following CL347 treatment, we performed flow cytometry on tumor cell suspensions. Briefly, live cells were sorted using and stained with CD11b, F4/80, and MHCII for macrophages quantification. As shown in Figure 4E and 4F, CL347 treatment significantly decreased the macrophage tumor content as compared to mock-treated tumors (-35%±12%, $p<0.05$). We analyzed tumor RNA content and found that the expression of chemokines involved in macrophage (CCL2, CCL7) and neutrophil (CXCL5) infiltration are down regulated in tumors treated by CL347, as

compared to mock-treated tumors (Supplemental Figure 4A). In pancreatic cancer, macrophages co-expressing costimulatory molecule CD86 and mannose receptor CD206 have been described as M2 anti-inflammatory macrophages, while those that only express the CD86 are most commonly associated with M1 pro-inflammatory properties[22]. We found that murine pancreatic tumors were mainly populated by CD86+/CD206+ macrophages (67%±2%, Figure 4G and 4H). On one hand, CL347 resulted in a significant decrease in CD86+/CD206+ macrophages content in experimental PDAC tumors (-30%, $p<0.05$, Figure 4G and 4I). Similarly, we found that the expression of Arg-1, that defines type II anti-inflammatory macrophages[23], is inhibited following CL347 treatment (Supplemental Figure 4B). On the other hand, CD86+/CD206- tumor associated macrophages significantly increases following CL347 administration, as compared to mock-treated tumors (37% *vs* 19%, $p<0.05$, Figure 4G and 4I). Previous studies have reported that the number of CD204-positive macrophages is related to tumor progression and clinical outcome in patients with PDAC[24]. Remarkably, CL347 treatment resulted in increased number of CD204-positive macrophages in experimental tumors, as compared to mock-treated mice (67% vs 57%, $p<0.05$). Thus, the pro-tumor effect of CL347 treatment is associated with the increase of CD86+/CD206-/CD204+ macrophages.

Last, we investigated the functional consequences of CL347 effect on the content and the phenotype of PDAC experimental tumors associated macrophages. Thus, mice with experimental tumors were treated with clodronate to deplete macrophages and treated with CL347 as described in Material and Methods. As shown in Figure 5A-C, clodronate treatment did not impacted experimental tumor growth. However, depleting macrophages strongly inhibited CL347 tumor growth (-63%, $p<0.05$, Figure 5B) and

viability (-87%, $p<0.01$ Figure 5C), demonstrating that CL347 pro-tumor effect is dependent on CD86+/CD206-/CD204+ pro-inflammatory M1 macrophages.

Collectively, our data demonstrate that TLR7 ligation inhibits PDAC cell proliferation *in vitro* and *in vivo* in immunodeficient models of PDAC. However, in immunocompetent experimental models closely resembling human disease, TLR7 activation provokes massive modification in the tumor associated macrophage content and phenotype that promote tumor progression and shortens mice survival.

Discussion

PDAC is one of the few deadly diseases that has not yet been defeated by immunotherapies[3]. In this context, TLR ligands are of high therapeutic interest as they show promising antitumoral activity either by directly inhibiting PDAC cell proliferation or inducing innate immune response against the tumor[12].

Unfortunately, multiple lines of evidence point to a more complex picture, with recent studies reporting opposite outcomes following treatment of experimental PDAC with TLR agonists. In this study, we confirm that TLR7 agonists have intrinsic antiproliferative and pro-apoptotic activities in cell lines. Noteworthy, we found that CL347 activity strictly depends on TLR7 expression in murine PDAC cells, and that CL347 treatment provokes major perturbations in cancer cells cell cycle, including profound inhibition of Cyclin E1 and Cyclin B1 expression. Cyclin E1 drives the transition from G1 to S phase by binding and activation of cyclin dependent kinase 2 (CDK2), resulting in the initiation of DNA synthesis, while Cyclin B1 is the regulatory subunit of M-phase promoting factor, and is essential for the initiation of mitosis. These data are in line with CL347-induced inhibition of cell proliferation, and also with previous reports describing the action of TLR7 agonists on PDAC cells[13]. In addition, we found that cdc2 and histone H3

phosphorylation is strongly inhibited by CL347, further indicating that progression into mitosis is strongly impaired in cells treated with TLR7 agonists. Last, we demonstrate during this study that CL347 treatment ultimately translates into tumor growth control in immunodeficient mice. Also, it is worth mentioning that CL347 TLR7 ligand also contains a lipid domain which could act as a nucleic-acid carrier. However, during this study, we failed to transfect therapeutic genes of interest with CL347 in PDAC derived cell lines (data not shown). In addition, such lipid structure may account for increased stability of CL347, that may lead to prolonged exposure to TLR7 agonists to induce unspecific cell death or even immune tolerance and immunosuppression.

In this study, we also highlight the Janus face of TLR7 on tumor growth as acute TLR7 ligands administration remodels the macrophage landscape of PDAC experimental tumors ultimately increasing tumor burden and shortening mice survival, regardless of the mode of administration. Thus, we report that despite a valuable inhibitory action on neoplastic cells, acute treatment with TLR7 agonists also promotes tumor supportive host immune response. We also provide the starkest possible reminder that PDAC tumors cannot be considered as an assembly of neoplastic cells, given the crucial importance of stromal reactions associated with this tumor type[2].

Our study is consistent with recent works from the literature illustrating that TLR7 activation may have opposite effect in PDAC models. As stated before, PDAC is an aggressive cancer that interacts with stromal cells to produce a highly inflammatory TME that promotes tumor growth and invasiveness. In an immunocompetent mouse model of PDAC, genetic ablation of TLR7 within inflammatory cells protects from neoplasia[15]. In a sibling study, Michaelis *et al.* remarkably demonstrated that host rather than neoplastic TLR7 is necessary for TLR agonists' beneficial antitumoral effect, notably after engagement of an antitumoral immune response[18]. These authors also raise substantial

awareness after showing that chronic administration of the TLR7 ligand R848 could also increase tumor growth[18], a situation we reproduced in the current study.

In this work, we shined a new light on the mode of action of TLR7 in murine models of PDAC. Indeed, we found that administration of TLR7 agonists decreases intratumoral T-cell infiltration and promotes F4/80-positive cells colonization of tumors. Deeper investigation demonstrates that TLR7 stimulation significantly decreases the number of macrophages in experimental tumors. One mechanistic explanation could be the decrease of MCP-1/CCL2 expression following CL347 treatment, as this cytokine mediates monocyte egress from bone marrow and recruitment into inflamed tissues through interaction with the CCR2 chemokine receptor[25]. Similarly, CL347 treatment resulted in decreased expression of CCL7 and CXCL5, that are both involved in neutrophil infiltration[26,27], including in PDAC[26]. Still, the molecular mechanisms involved in such regulation are still unknown and require further investigation.

We next investigated the macrophage landscape of tumors treated by CL347. On one hand, we found that TLR7 agonists induce a pro-inflammatory, CD86-positive and CD206-negative, M1-like phenotype, and decreases the proportion of anti-inflammatory, M2-like cells expressing both CD86 and CD206. On the other hand, we found that CL347 augments the percentage of macrophages expressing CD204. Remarkably, CD204 macrophages have been associated with tumor-promoting effects in pancreatic cancer by inducing Th2 and regulatory T cell (Treg) differentiation of CD4+ T cells[28] and are associated with a worst prognosis and early disease recurrence[29] in PDAC patients. During this study, we demonstrate that macrophages are the cornerstone of CL347 deleterious effect on PDAC tumors, as macrophage depletion largely blunts CL347-induced pro-tumoral effect. This may suggest that pro-inflammatory M1-like TAM can also exert several pro-tumoral functions following TLR7 activation. Of importance, PDAC

often originates from inflammatory disease such as pancreatitis, that is known to accelerate carcinogenesis in animal models for this disease[30]. Here, CL347 treatment may induce a "supra-inflammatory" state in tumors to flourish, by promoting macrophages with distinct pro-inflammatory and pro-tumoral phenotype. Hence, the current study may suggest that generally accepted dichotomous M1-versus-M2 classification fails to capture the ontogeny and tissue-specific cues and stress responses of highly plastic TAM, and should be rather considered as a gradient. Future studies using single-cell RNAseq will help better understand the molecular changes in macrophages consecutive to TLR7 treatment of murine PDAC tumors. Hence, our study faces limitations as in humans, TLR7 is predominantly expressed in plasmacytoid dendritic cells and B cells, with context dependent expression in a subset of T cells[22]. This may result in very distinct profiles of cytokines secretion following TLR7 activation. One could expect that pro-tumoral cytokines such as IL-6 would be much less induced[31], while type-1 IFN signaling may prevail to favor tumor inhibition, as we found before[32]. Further studies based on samples from patients with PDAC treated by TLR7 agonisits are needed to better address this concern.

Finally, it would be of interest to determine the origin of TAMs involved in CL347 protumoral effect. We found that TLR7 activation decreases the number of TAM, strongly suggesting that monocyte recruitment is inhibited following treatment. Such finding points towards a role of tissue resident-macrophages in CL347-induced tumor promotion. This is of particular importance as a recent report nicely demonstrated that tissue-resident macrophages are an essential source of tumor promoting macrophages in murine PDAC models[26]. Such embryonically derived TAMs exhibit a pro-fibrotic transcriptional profile, indicative of their role in producing and remodeling molecules in the extracellular matrix[26,] that may further support tumor growth.

Taken together, our results highlight the importance of evaluating candidate molecules using animal models that faithfully recapitulate tumors in patients, as therapeutic outcome must be conceived of as the sum of effects on the cancer cells and the host (TME) in which the disease takes place. Here, we report for the first time the duality of action of TLR7 agonists in experimental PDAC models, and call into question the use of TLR7 agonists for PDAC therapy.

Materials and methods

Reagents. PAM3CSK4 (TLR1/2 agonist), SSRNA-40 (TLR7/8 agonist), CL264 (TLR7 agonist), CL307 (TLR7 agonist coupled with spermine to enhance cellular uptake by endocytosis), CL347 (TLR7 agonist derived from CL307 by conjugation with a bis(phytanyl) phosphonate group for nucleic acid transfection), CL419 (TLR2 agonist coupled with spermine and conjugated with a bis(phytanyl) phosphonate group for nucleic acid transfection) and CL553 (TLR2/7 agonist coupled with spermine and conjugated with a bis(phytanyl) phosphonate group for nucleic acid transfection) were purchased from Invivogen (Toulouse, France). A complete description of the different compounds' affinity and efficacy is available at www.invivogen.com. Lentiviral plasmids encoding for Red-shifted luciferase (RediFect Red-Shifted FLuc, RSLucF) or for NucLight Green (NucG) were from Perkin Elmer (Waltham, MA, USA) and Sartorius (Essen Biosciences, Hertfordshire, UK), respectively. Control plasmids and plasmids expressing small interfering RNA against murine TLR7 were from Invivogen (Toulouse, France). JetPRIME was purchased from Polyplus (Illkirch-Graffenstaden). Antibodies used in this study were from Cell Signaling Technology (total PARP, ref. 9532, cleaved PARP ref. 5625, β-actin ref. 8H10D10 and cell cycle phase determination antibody

sampler kit, ref. 17498) and used following the manufacturer's recommendation (Cell Signaling Technology, Danvers, Massachusetts, USA).

Cell culture. All murine pancreatic cancer cells are kind gifts of D. Sauer (TUM, Munich, Germany). R211 cells derive from spontaneous tumors generated in the KPC mice model (LSL-KrasG12D/+; LSL-Trp53R172H/+; Pdx-1-Cre). DT6606 cells derive from spontaneous tumors generated in the KC mice model (LSL-KrasG12D/+; Pdx-1-Cre). PKP16 cells derive from spontaneous tumors generated in the KP16C mice model (LSL-KrasG12D/+; LSL-Tp16/INK4A/+; Pdx-1-Cre). Mia PACA-2, Capan-1, Capan-2, BxPC-3 and Panc-1 cells were purchased from LGC standards (Molsheim, France). Cells were grown in DMEM 4.5g/L glucose medium supplemented with 10% fetal calf serum (FCS), L-glutamine, antibiotics (Life Technologies) and plasmocyn (Invivogen, complete medium) at 37°C in humid atmosphere with 5% CO2. Cell cultures were certified mycoplasma-free (PlasmoTest kit, Invivogen).

Lentiviral transduction and cell transfection. For lentiviral transduction, R211 cells were seeded at a density of 10^4 cells per well in a 48 well-dish. After 24h, cells were incubated with 150 ng of p24-equivalent of lentiviral vectors in the presence of protamine sulfate (4 µg/mL) for 16h. Transduced cells were selected for 3 weeks using puromycin (5 µg/mL,-InvivoGen) or Zeocin (100 ng/ml, Invivogen) when transduced with RSLucF, or NucG lentiviral vectors, respectively. For cell transfection, R211 cells were seeded in 96-well plates or 60-mm dishes and transfected with 100ng or 500ng of plasmid DNA (psiRNA-TLR, reference ksirna42-mtlr7, Invivogen) and JetPRIME, respectively, according to the manufacturer instructions.

Cell proliferation. IncuCyte ZOOM Live-Cell Imaging system (Sartorius, Goettingen, Germany) was used for kinetic monitoring of cell proliferation and cytotoxicity of TLR agonists in murine pancreatic cancer cells. Briefly, R211-NucG cells were seeded at 10^4/well in 96-well black-walled plates. Cells were treated with increasing concentrations (12.5-100 µM) of TLR agonists in complete medium in the presence of IncuCyte® Cytotox Red (Sartorius), following the manufacturer's recommendation. R211 nucleus is labelled in green, and IncuCyte® Cytotox Red labels dead cells yielding red fluorescence. The plate was scanned, and fluorescent and phase-contrast images were acquired in real time every hour from 0 to 72 hours post treatment. Normalized Green and Red Object Count per well at each time point were generated by IncuCyte ZOOM software and plotted using GraphPad Prism v8.3.1 (549) (Graphpad Software, San Diego, CA, USA). Representative pictures and mask are shown in supplemental Figure 1A-D.

For cell counting studies, DT6606, PKP16 and Mia PACA-2 cells were seeded in triplicate at a concentration of 5.10^4/well of 6 well-plates. After 24h (t=0), cells were counted using a Z1 Coulter® Particle Counter (Beckman Coulter, Pasadena, California, USA), then treated with TLR ligands at the indicated dose. Cells were subsequently counted after 72h in culture.

Western blotting. Cell pellets were incubated in RIPA buffer supplemented with 10 µL/mL protease inhibitor (Sigma-Aldrich, Saint-Louis, Missouri, USA). After 15 min on ice, samples are centrifuged (15 min-12 000rpm, 4°C). Protein fractions were denaturated in Laemmli buffer after heating at 95°C for 5 min. Proteins were separated by SDS-PAGE (Sodium Dodecyl Sulfate Polyacrylamide Gel Electrophoresis) and transferred onto nitrocellulose membrane (Bio-Rad) using TransBlot Turbo apparatus

(Bio-Rad, Hercules, California, USA). After membrane saturation and primary/secondary antibody incubation, protein expression was detected using ClarityTM Western ECL Substrate (Bio-Rad) and Chemi-DocTM XRS+ (Bio-Rad) apparatus. Signal intensities were quantified using Image Lab (Bio-Rad) software.

Flow cytometry. For cell cycle analyses, cells were fixed in 70% ethanol during the exponential growth. Fixed cells were treated with RNAse A (10 µg/mL) and propidium iodide (20 µg/mL) (Sigma-Aldrich) for 15 min at 37°C. Data were acquired using the MACS Quant® VYB cytometer (Miltenyi Biotech, Bergisch Gladbach Germany) and analyzed with MACS Quant and ModFit software. For the analysis of the intratumoral macrophage content, single-cell suspensions from tumor tissue were generated using the tumor dissociation kit (mouse, Myltenyi Biotec). Live cells were sorted using the LIVE/DEAD Fixable Aqua Dead Cell Stain Kit (ThermoFisher scientific, Waltham, Massachusetts, USA), and FITC-CD11b, APC-F4/80, PerCP Vio700-MHCII, PE-CD86, RPE Alexa750-CD206 and VioBlue-CD204 antibodies were used to characterize tumor-associated macrophages. Corresponding isotype controls were used as negative controls. All antibodies were from Miltenyi, with the exception of anti-CD206 RPE 750 antibody (Serotec, Bio-Rad, Hercules, CA).

Gene expression analysis. For Quantitative reverse transcription PCR studies (RT-qPCR), total RNA was isolated cell lines with TRIzol® Reagent (Life Technologies) according to supplier's instructions. One to five µg of total RNA were reverse transcribed into cDNA using RevertAid H minus Reverse Transcriptase kit (ThermoFisher scientific) according to manufacturer's recommendations. Duplicate RT-qPCR assays were carried out in a StepOnePlus™ Real-Time PCR System (Applied Biosystems, Waltham, Massachusetts, USA) with SsoFast™ EvaGreen® supermix (Bio-Rad) and specific

primers (see primers listed in Supplemental Materials and Methods 2). Relative quantity of mRNA was calculated by the comparative threshold cycle (CT) method as $2^{-\Delta CT}$, where ΔCT = CT *candidate gene* mRNA – CT *Reference* mRNA. *β-Actin* was used for normalization. Primers for TLR2 and TL7 expression studies are the following: human TLR2-Forward: TTG ATG ACT CTA CCA GAT GCC, human TLR2-Reverse: CAA ATG AAG TTA TTG CCA CCA G, human TLR7-Forward: TCT GAC TAA CCT GAT TCT GTT CTC, human TLR7-Reverse: GTG ATA TTA GAC GCT GAT ACC C, murine TLR2-Forward: GTC TTT CAC CTC TAT TCC CTC C, murine TLR2-Reverse: CCC TCT ATT GTA TTG ATT CTG CTG, murine TLR7-Forward: CGG TGA TAA CAG ATA CTT GGA C, murine TLR7-Reverse: AGA GAT TCT TTA GAT TTG GCG G.

For Nanostring quantification of gene expression, tumors were sampled and minced in liquid nitrogen. Total RNA was extracted with TRIzol® Reagent (Life Technologies) according to supplier's instructions. One hundred nanograms of RNA were analyzed using the murine inflammation panel according to supplier's instructions. Genes with reads below 50 were not further considered. Raw data from Nanostring was performed using the NanoStringDiff package (NanoStringDiff_1.14.0 Biobase_2.44.0). Differential Gene Expression analysis was conducted using the package (see process_nanostringFinal.R). Volcano plots were generated with Enhanced Volcano package (EnhancedVolcano_1.2.0). We performed enrichment analysis using ToppGene, accessed on 19th July 2019[33].

***In vivo* experiments.**

Experimental procedures performed on mice were approved by the ethical committee of INSERM CREFRE US006 animal facility and authorized by the French Ministry of Research: APAFIS#3600-2015121608386111v3. R211-RSLucF cells (5.10^4 cells) were

injected into the pancreas of NOD scid gamma (NSG) or C57bl6 mice (n=6 per group). Tumor growth monitoring was performed non-invasively twice a week by injecting Xenolight D-Luciferin (Perkin Elmer, Waltham, Massachusetts, USA) and recording relative light units (r.l.u.) using the Ivis Spectrum (Perkin Elmer), following the manufacturer's recommendations. Additionally, tumor volume was measured using the Aixplorer apparatus (Supersonic Imagine, Aix-en-Provence, France). Ten to 15 days following tumor induction, mice with exponentially growing tumors were injected intraperitoneally with 100µl of either placebo (PBS with 5% glucose), CL347 and R848 diluted in PBS with 5% glucose at the indicate dose. Tumor growth was monitored non-invasively as mentioned before at the indicated time point. Mice were killed 15 (immunodeficient model) to 25 (immunocompetent model) days following treatment.

Immunohistochemistry.

Tumors were harvested and fixed in formalin. Four-micrometer-thick sections were prepared from paraffin-embedded sections and rehydrated. Ki67 staining was performed as previously described[34]. For TLR7 and CD3 staining, antigen retrieval was performed using 10mM Tris-HCl pH 8.5 or Tris-EDTA, respectively. Slides were incubated 3 hours at room temperature with TLR7 antibodies (Novus Biologics, Centennial, CO 80112, USA , ref. NBP2 24906) diluted 1:100 or CD3 antibodies (Spring biosciences, Pleasanton, CA 94588, USA, Clone SP7, ref. M3070) diluted 1:200 in Antibody diluent solution (DakoCytomation, Santa Clara, CA, USA). After several washes in PBS, EnVision+ System- HRP labelled polymer anti-rabbit were added as per requested by the manufacturer (DakoCytomation), followed by horseradish peroxidase streptavidin (dilution 1:500, SA-5004, Vector, Burlingame, CA, USA). Slides were quickly washed twice in PBS and incubated in AEC+ reagent and counterstained with Mayer's

hematoxylin (DakoCytomation). After washing in PBS, slides were mounted with Vectashield (Vector). Immunostaining was recorded with an AXIO optical microscope (Zeiss) equiped with a colour AXIOCAM camera 105 (Zeiss, Oberkochen, Germany) and quantified using ImageJ.

Statistical analysis

Data were analysed by 2-tailed, unpaired Student's t-test using a multiple statistics Graph Pad Prism 8 software package and a difference was considered significant when p value was lower than 0.05. Mean values are given ± SD. Number of independent experiments is indicated in the figure legends. *, ** and *** indicate a p value < 0.05, <0.01 and <0.001, respectively. For Nanostring data analysis, we analysed first the genes that were highest in logFC (top30) irrespective of p-val and then gene that were Up and had p-val <0.1.

Acknowledgments.

This work was supported by grants from Region Occitanie (grant number 13053110 and 15052181) and CHU Toulouse (M.R.). The authors would like to thank Dr. M. Dufresne for immunohistochemistry protocols and Drs. F. Vernejoul, M. Vienne and J. Torrisani for helpful discussions. The authors would like to thanks Ms E. Martin for technical help. We acknowledge the Phenotyping department of the CREFRE-Anexplo platform, and more specifically Laurent Monbrun for his technical assistance.

Author Contributions

Conceptualization, P.C., A.C. and L.B.; investigations M.R., P.G., G.J., C. F., N. H., H.L., E.S., C.V., and M.S.; supervision, P.C.; writing – original draft, P.C.; writing – review &

editing F.L., A.C., G.J., L.B., M.S. and V.P.; funding acquisition, P.C.; data analysis, L.B., P.C., A.C., G.J., N.H., M.S, M.R., V.P. and F.L.

TABLES

Product	ssRNA40	PAM3CSK4	R848	CL264	CL307	CL347	CL419	CL553
Target	hTLR8-mTLR7	TLR1/2	TLR7/8	TLR7	TLR7	TLR7	TLR2	TLR2/7
IC50 (µM)	302	57	250	159	104	77	116	121
SD (IC50)	1,42	1,19	2,5	1,22	1,1	1,25	1,3	1,23

Table 1 : antiproliferative efficacy of natural and synthetic TLR agonists in primary, murine pancreatic cancer cells. Results are mean of three independent experiments performed in sextuplet.

REFERENCES

1. Rahib, L., Smith, B.D., Aizenberg, R., Rosenzweig, A.B., Fleshman, J.M., and Matrisian, L.M. (2014). Projecting Cancer Incidence and Deaths to 2030: The Unexpected Burden of Thyroid, Liver, and Pancreas Cancers in the United States. Cancer Res. *74*, 2913–2921.
2. Kleeff, J., Korc, M., Apte, M., La Vecchia, C., Johnson, C.D., Biankin, A.V., Neale, R.E., Tempero, M., Tuveson, D.A., Hruban, R.H., et al. (2016). Pancreatic cancer. Nat. Rev. Dis. Primer *2*, 16022.
3. Neoptolemos, J.P., Kleeff, J., Michl, P., Costello, E., Greenhalf, W., and Palmer, D.H. (2018). Therapeutic developments in pancreatic cancer: current and future perspectives. Nat. Rev. Gastroenterol. Hepatol. *15*, 333–348.
4. Huang, B., Zhao, J., Unkeless, J.C., Feng, Z.H., and Xiong, H. (2008). TLR signaling by tumor and immune cells: a double-edged sword. Oncogene *27*, 218–224.
5. Pushalkar, S., Hundeyin, M., Daley, D., Zambirinis, C.P., Kurz, E., Mishra, A., Mohan, N., Aykut, B., Usyk, M., Torres, L.E., et al. (2018). The Pancreatic Cancer Microbiome Promotes Oncogenesis by Induction of Innate and Adaptive Immune Suppression. Cancer Discov. *8*, 403–416.
6. De Nardo, D. (2015). Toll-like receptors: Activation, signalling and transcriptional modulation. Cytokine *74*, 181–189.
7. Shi, M., Chen, X., Ye, K., Yao, Y., and Li, Y. (2016). Application potential of toll-like receptors in cancer immunotherapy: Systematic review. Medicine (Baltimore) *95*, e3951.
8. Feng, Y., Mu, R., Wang, Z., Xing, P., Zhang, J., Dong, L., and Wang, C. (2019). A toll-like receptor agonist mimicking microbial signal to generate tumor-suppressive macrophages. Nat. Commun. *10*, 1–14.
9. Perkins, D.J., and Vogel, S.N. (2015). Space and time: New considerations about the relationship between Toll-like receptors (TLRs) and type I interferons (IFNs). Cytokine *74*, 171–174.
10. Zahm, C.D., Colluru, V.T., McIlwain, S.J., Ong, I.M., and McNeel, D.G. (2018). TLR Stimulation during T-cell Activation Lowers PD-1 Expression on CD8+ T Cells. Cancer Immunol. Res. *6*, 1364–1374.
11. Kobold, S., Wiedemann, G., Rothenfußer, S., and Endres, S. (2014). Modes of action of TLR7 agonists in cancer therapy. Immunotherapy *6*, 1085–1095.
12. Santoni, M., Andrikou, K., Sotte, V., Bittoni, A., Lanese, A., Pellei, C., Piva, F., Conti, A., Nabissi, M., Santoni, G., et al. (2015). Toll like receptors and pancreatic diseases: From a pathogenetic mechanism to a therapeutic target. Cancer Treat. Rev. *41*, 569–576.
13. Zou, B.-B., Wang, F., Li, L., Cheng, F.-W., Jin, R., Luo, X., Zhu, L.-X., Geng, X., and Zhang, S.-Q. (2015). Activation of Toll-like receptor 7 inhibits the proliferation and migration, and induces the apoptosis of pancreatic cancer cells. Mol. Med. Rep. *12*, 6079–6085.
14. Grimmig, T., Matthes, N., Hoeland, K., Tripathi, S., Chandraker, A., Grimm, M., Moench, R., Moll, E.-M., Friess, H., Tsaur, I., et al. (2015). TLR7 and TLR8 expression increases tumor cell proliferation and promotes chemoresistance in human pancreatic cancer. Int. J. Oncol. *47*, 857–866.
15. Ochi, A., Graffeo, C.S., Zambirinis, C.P., Rehman, A., Hackman, M., Fallon, N., Barilla, R.M., Henning, J.R., Jamal, M., Rao, R., et al. (2012). Toll-like receptor 7 regulates pancreatic carcinogenesis in mice and humans. J. Clin. Invest. *122*, 4118–4129.
16. Narayanan, J.S.S., Ray, P., Hayashi, T., Whisenant, T.C., Vicente, D., Carson, D.A., Miller, A.M., Schoenberger, S.P., and White, R.R. (2019). Irreversible Electroporation Combined with Checkpoint Blockade and TLR7 Stimulation Induces Antitumor Immunity in a Murine Pancreatic Cancer Model. Cancer Immunol. Res. *7*, 1714–1726.
17. Schölch, S., Rauber, C., Tietz, A., Rahbari, N.N., Bork, U., Schmidt, T., Kahlert, C., Haberkorn, U., Tomai, M.A., Lipson, K.E., et al. (2015). Radiotherapy combined with TLR7/8 activation induces strong immune responses against gastrointestinal tumors. Oncotarget *6*, 4663–4676.
18. Michaelis, K.A., Norgard, M.A., Zhu, X., Levasseur, P.R., Sivagnanam, S., Liudahl, S.M., Burfeind, K.G., Olson, B., Pelz, K.R., Angeles Ramos, D.M., et al. (2019). The TLR7/8 agonist R848 remodels tumor and host responses to promote survival in pancreatic cancer. Nat. Commun. *10*, 4682.
19. Calore, F., Londhe, P., Fadda, P., Nigita, G., Casadei, L., Marceca, G.P., Fassan, M., Lovat, F., Gasparini, P., Rizzotto, L., et al. (2018). The TLR7/8/9 Antagonist IMO-8503 Inhibits Cancer-Induced Cachexia. Cancer Res. *78*, 6680–6690.

20. Gutjahr, A., Papagno, L., Nicoli, F., Lamoureux, A., Vernejoul, F., Lioux, T., Gostick, E., Price, D.A., Tiraby, G., Perouzel, E., et al. (2017). Cutting Edge: A Dual TLR2 and TLR7 Ligand Induces Highly Potent Humoral and Cell-Mediated Immune Responses. J. Immunol. Baltim. Md 1950 *198*, 4205–4209.
21. Hingorani, S.R., Wang, L., Multani, A.S., Combs, C., Deramaudt, T.B., Hruban, R.H., Rustgi, A.K., Chang, S., and Tuveson, D.A. (2005). Trp53R172H and KrasG12D cooperate to promote chromosomal instability and widely metastatic pancreatic ductal adenocarcinoma in mice. Cancer Cell *7*, 469–483.
22. Villalobos-Ayala, K., Ortiz Rivera, I., Alvarez, C., Husain, K., DeLoach, D., Krystal, G., Hibbs, M.L., Jiang, K., and Ghansah, T. (2020). Apigenin Increases SHIP-1 Expression, Promotes Tumoricidal Macrophages and Anti-Tumor Immune Responses in Murine Pancreatic Cancer. Cancers *12*, E3631.
23. Arlauckas, S.P., Garren, S.B., Garris, C.S., Kohler, R.H., Oh, J., Pittet, M.J., and Weissleder, R. (2018). Arg1 expression defines immunosuppressive subsets of tumor-associated macrophages. Theranostics *8*, 5842–5854.
24. Kurahara, H., Shinchi, H., Mataki, Y., Maemura, K., Noma, H., Kubo, F., Sakoda, M., Ueno, S., Natsugoe, S., and Takao, S. (2011). Significance of M2-polarized tumor-associated macrophage in pancreatic cancer. J. Surg. Res. *167*, e211-219.
25. Sierra-Filardi, E., Nieto, C., Domínguez-Soto, A., Barroso, R., Sánchez-Mateos, P., Puig-Kroger, A., López-Bravo, M., Joven, J., Ardavín, C., Rodríguez-Fernández, J.L., et al. (2014). CCL2 shapes macrophage polarization by GM-CSF and M-CSF: identification of CCL2/CCR2-dependent gene expression profile. J. Immunol. Baltim. Md 1950 *192*, 3858–3867.
26. Chao, T., Furth, E.E., and Vonderheide, R.H. (2016). CXCR2-Dependent Accumulation of Tumor-Associated Neutrophils Regulates T-cell Immunity in Pancreatic Ductal Adenocarcinoma. Cancer Immunol. Res. *4*, 968–982.
27. Ford, J., Hughson, A., Lim, K., Bardina, S.V., Lu, W., Charo, I.F., Lim, J.K., and Fowell, D.J. (2018). CCL7 Is a Negative Regulator of Cutaneous Inflammation Following Leishmania major Infection. Front. Immunol. *9*, 3063.
28. Liu, C.-Y., Xu, J.-Y., Shi, X.-Y., Huang, W., Ruan, T.-Y., Xie, P., and Ding, J.-L. (2013). M2-polarized tumor-associated macrophages promoted epithelial-mesenchymal transition in pancreatic cancer cells, partially through TLR4/IL-10 signaling pathway. Lab. Investig. J. Tech. Methods Pathol. *93*, 844–854.
29. Okubo, S., Suzuki, T., Hioki, M., Shimizu, Y., Toyama, H., Morinaga, S., Gotohda, N., Uesaka, K., Ishii, G., Takahashi, S., et al. (2021). The immunological impact of preoperative chemoradiotherapy on the tumor microenvironment of pancreatic cancer. Cancer Sci.
30. Buscail, L., Bournet, B., and Cordelier, P. (2020). Role of oncogenic KRAS in the diagnosis, prognosis and treatment of pancreatic cancer. Nat. Rev. Gastroenterol. Hepatol.
31. Gorden, K.B., Gorski, K.S., Gibson, S.J., Kedl, R.M., Kieper, W.C., Qiu, X., Tomai, M.A., Alkan, S.S., and Vasilakos, J.P. (2005). Synthetic TLR agonists reveal functional differences between human TLR7 and TLR8. J. Immunol. Baltim. Md 1950 *174*, 1259–1268.
32. Ravet, E., Lulka, H., Gross, F., Casteilla, L., Buscail, L., and Cordelier, P. (2010). Using lentiviral vectors for efficient pancreatic cancer gene therapy. Cancer Gene Ther. *17*, 315–324.
33. Chen, J., Bardes, E.E., Aronow, B.J., and Jegga, A.G. (2009). ToppGene Suite for gene list enrichment analysis and candidate gene prioritization. Nucleic Acids Res. *37*, W305-311.
34. Sicard, F., Gayral, M., Lulka, H., Buscail, L., and Cordelier, P. (2013). Targeting miR-21 for the therapy of pancreatic cancer. Mol. Ther. J. Am. Soc. Gene Ther. *21*, 986–994.

FIGURE LEGENDS

Figure 1. Antiproliferative and proapoptotic activity of TLR7 ligands CL347 in pancreatic cancer cells. A. R211 cells derived from spontaneous murine pancreatic tumors and genetically engineered to express fluorescent nuclear reporter (R211-NucGreen) were treated in 96-well plates with CL347 at the indicated dose. Control cells were treated with medium only or TLR agonist solvent (water, ethanol). Cells nuclei were imaged and numbered non-invasively every hour for three days using the Incucyte Zoom as described in Materials and Methods. Results are mean ± SD of triplicates and representative of three independent experiments. **B.** R211-NucGreen cells were treated with 100µm of PAMS3CSK4, CL264, SSRNA-40, CL307, CL419, CL347 and CL553. Control cells were treated with medium only or TLR agonist solvent (water, ethanol). Cells were incubated with cytotox red reagent for counting dead cells non-invasively every hour for three days using the Incucyte Zoom as described in Materials and Methods. Results are mean ± SD of triplicates and representative of three independent experiments. **C**. R211-NucG cells were transfected with plasmid DNA encoding for specific hairpins against mTLR7. As control, cells were transfected with plasmid expressing control random hairpins. Cells were treated with CL347 at the indicated dose and cell proliferation was measured using the Incucyte Zoom. Results are mean ± SD of 4 to 6 replicates per group and representative of three independent experiments. **D**. Murine PDAC DT6606 cells and Human PDAC Mia PACA-2 cells were treated for 48 hours with 50µM of CL347 and analyzed for cell cycle phase distribution by fluorescence-activated cell sorting. Results are mean ± SD of three independent experiments. R211-NucG cells were seeded in 100-mm dishes and treated with 50µm of CL347 for forty-eight hours. Cells were lysed and soluble proteins were analyzed by

Western blot for the indicated cell cycle protein (**E**) or protein involved in apoptosis (**F**). β-actin and HSP90 are used as loading control. Quantification is indicated (fold variation vs Mock). Representative of three independent experiments. **: $p<0.01$, ***: $p<0.005$

Figure 2. Antitumoral activity of CL347 TLR7 ligands in immunodeficient models of pancreatic cancer. R211 cells were genetically engineered to express Red-shifted luciferase reporter gene (R211-RSLuc) and engrafted in the pancreas of athymic (NOD scid gamma) mice as described in Materials and Methods. Fifteen days following engraftment, mice received PBS placebo or CL347 I.P. at the indicated dose in 100µl of 5% glucose intraperitoneally. As control, mice were injected with 100µl of PBS with 5% glucose. Five to six mice were used per group. **A**. Survival rate in control and mice treated with CL347. **B**. Tumor growth was monitored non-invasively using the Ivis spectrum and quantified as tumor viability expressed as relative light units (r.l.u.) using Living image software. **C**. Representative Ki67 staining in control and mice treated by 80µg of CL347, 15 days following treatment. Scale bar: 100µm. **D**. Quantification of Ki-67 positive cells per field in control and mice treated by 80µg of CL347. Results are mean ± S.D. of ten fields from three different tumors. **: $p<0.01$, ***: $p<0.005$.

Figure 3. TLR7 ligands treatment accelerate pancreatic carcinogenesis in immunocompetent mice. R211-RSLuc cells were engrafted in the pancreas of C57/BL6 mice as described in Material and Methods. Fifteen days following engraftment, mice received PBS placebo or CL347 I.P. at the indicated dose in 100µl of 5% glucose. As control, mice were injected with 100µl of 5% glucose. Five to six mice were used per group. **A**. Survival rate in control and mice treated with CL347. **B**.

Representative Ki67 staining in control and mice treated by 80µg of CL347. Scale bar: 100µm. **C**. Quantification of Ki-67 positive cells per field in control and mice treated by 80µg of CL347. Results are mean ± S.D. of ten fields from three different tumors. **D**. MC57/BL6 with orthotopic R211-RSLuc tumors were treated as indicated. Three to four mice were used per group. Tumor growth was monitored non-invasively using the Ivis spectrum and quantified and tumor progression was expressed as relative light units (r.l.u.) using Living image software. *: $p<0.05$, **: $p<0.01$, ***: $p<0.005$

Figure 4. TLR7 ligands alters the immune landscape of murine PDAC tumors.

R211-RSLuc cells were engrafted in the pancreas of C57/BL6 mice as described in Material and Methods. Fifteen days following engraftment, mice received PBS placebo or 80µg CL347 I.P. in 100µl of 5% glucose. As control, mice were injected with 100µl of 5% glucose. Three to five mice were used per group. **A**. Representative CD3 staining in control and mice treated by CL347. Scale bar: 100µm. **B**. Quantification of CD3 positive cells per field in control and mice treated by 80µg of CL347. Results are mean ± S.D. of ten fields from three different tumors. **C**. Representative F4/80 staining in control and mice treated by CL347. Scale bar: 100µm. **D**. Quantification of F4/80 positive cells per field in control and mice treated by 80µg of CL347. Results are mean ± S.D. of ten fields from three different tumors. **E**. Representative FACS analysis of CD11b, F4/80, and MHCII-positive cells in control tumors and tumors treated by CL347. **F.** Quantification of CD11b, F4/80, and MHCII-positive cells in control tumors and tumors treated by CL347. Results are mean± S.D. of four tumors. **G**. Representative FACS analysis of CD86 and CD206 expression on macrophages from control tumors and tumors treated by CL347. **H-I**. Quantification of CD86 and CD206 expression on macrophages from control tumors

and tumors treated by CL347. Results are mean± S.D. of three and five tumors respectively. **J**. Representative FACS analysis of CD204 expression on macrophages from control tumors and tumors treated by CL347. **K**. Quantification of CD204 expression on macrophages from control tumors and tumors treated by CL347. Results are mean± S.D. of three and five tumors, respectively. *: $p<0.05$, **: $p<0.01$, ***: $p<0.005$.

Figure 5. Macrophages are essential to the protumoral effect of TLR7 ligands on murine PDAC tumors.

R211-RSLuc cells were engrafted in the pancreas of C57/BL6 mice and treated by clodronate and/or CL347 as described in Material and Methods. Three mice were used per group. Tumor growth was analyzed non-invasively using the Ivis Spectrum. **A**. Representative caption of tumor bioluminescence before and after 7 days of treatment as indicated. Mice were killed and tumor volume (**B**) and viability (**C**) were analyzed. *: $p<0.05$, **: $p<0.01$ (one-tailed t-test).

Figure 1

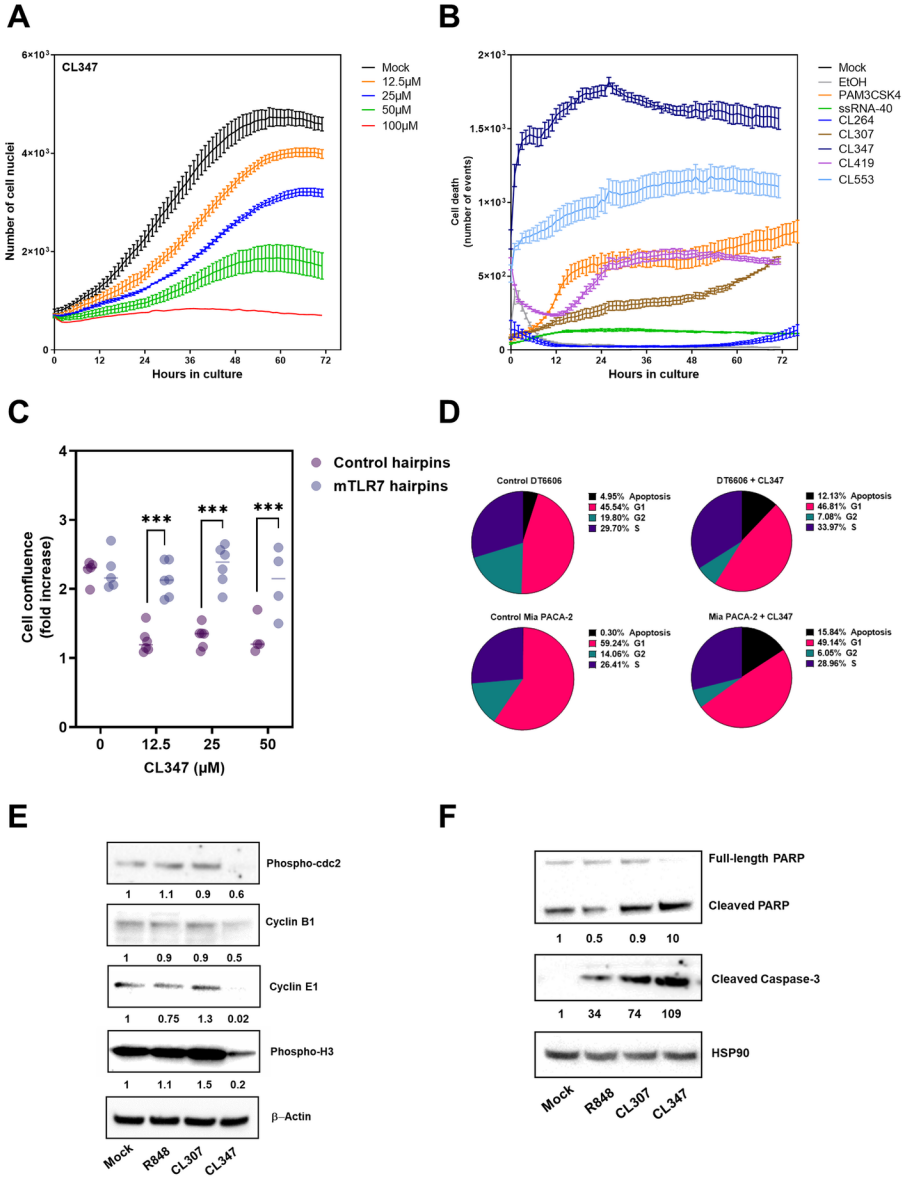
A
CL347
Number of cell nuclei
Hours in culture
Mock
12.5μM
25μM
50μM
100μM
B
Cell death (number of events)
Hours in culture
Mock
EtOH
PAM3CSK4
ssRNA-40
CL264
CL307
CL347
CL419
CL553
C
Cell confluence (fold increase)
CL347 (μM)
Control hairpins
mTLR7 hairpins
***
D
Control DT6606
4.95% Apoptosis
45.54% G1
19.80% G2
29.70% S
DT6606 + CL347
12.13% Apoptosis
46.81% G1
7.08% G2
33.97% S
Control Mia PACA-2
0.30% Apoptosis
59.24% G1
14.06% G2
26.41% S
Mia PACA-2 + CL347
15.84% Apoptosis
49.14% G1
6.05% G2
28.96% S
E
Phospho-cdc2
1 1.1 0.9 0.6
Cyclin B1
1 0.9 0.9 0.5
Cyclin E1
1 0.75 1.3 0.02
Phospho-H3
1 1.1 1.5 0.2
β--Actin
Mock
R848
CL307
CL347
F
Full-length PARP
Cleaved PARP
1 0.5 0.9 10
Cleaved Caspase-3
1 34 74 109
HSP90
Mock
R848
CL307
CL347

Figure 2

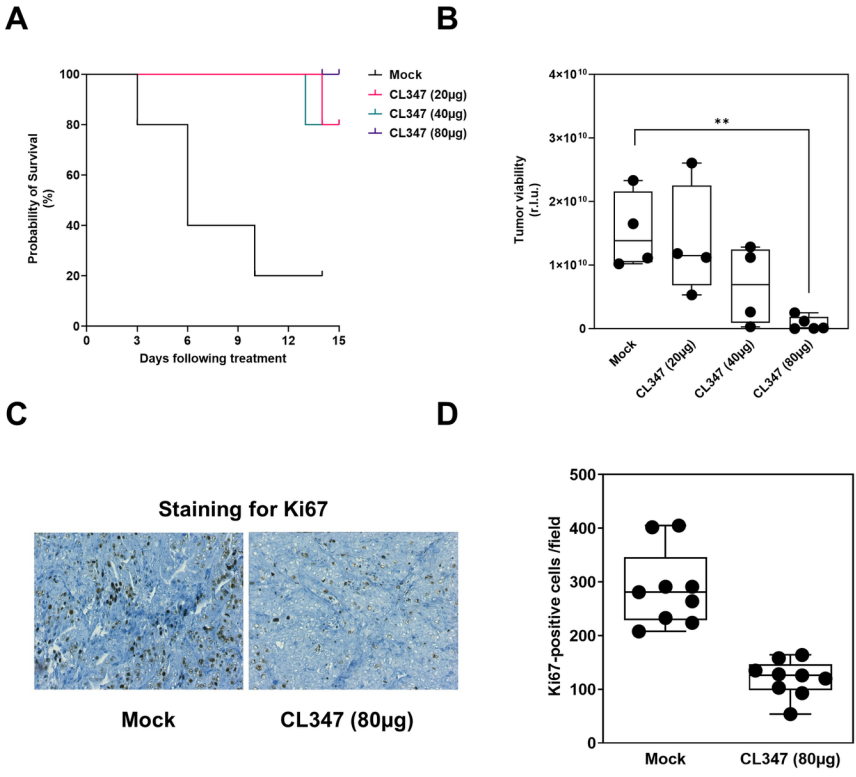
A
B
C
D
Probability of Survival (%)
Days following treatment
Mock
CL347 (20μg)
CL347 (40μg)
CL347 (80μg)
Tumor viability (r.l.u.)
**
Staining for Ki67
Mock
CL347 (80μg)
Ki67-positive cells /field

Figure 3

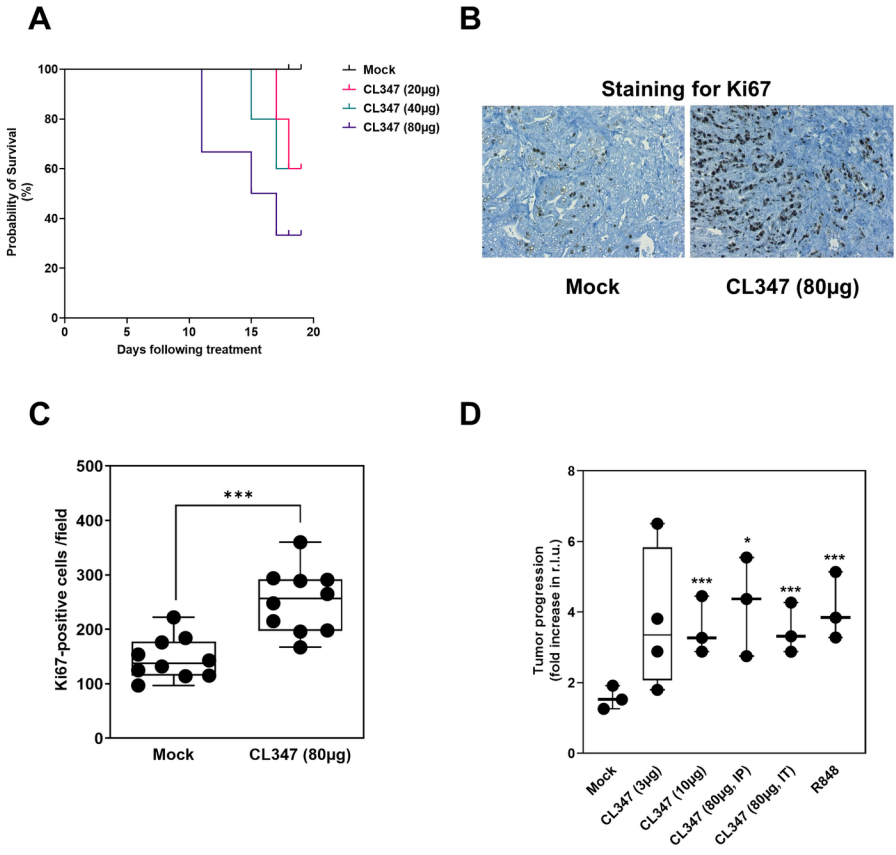
A
Probability of Survival (%)
100
80
60
40
20
0
0
5
10
15
20
Days following treatment
Mock
CL347 (20µg)
CL347 (40µg)
CL347 (80µg)
B
Staining for Ki67
Mock
CL347 (80µg)
C
Ki67-positive cells /field
500
400
300
200
100
0
***
Mock
CL347 (80µg)
D
Tumor progression (fold increase in r.i.u.)
8
6
4
2
0
***
*
***
***
Mock
CL347 (3µg)
CL347 (10µg)
CL347 (80µg, IP)
CL347 (80µg, IT)
R848

Figure 4

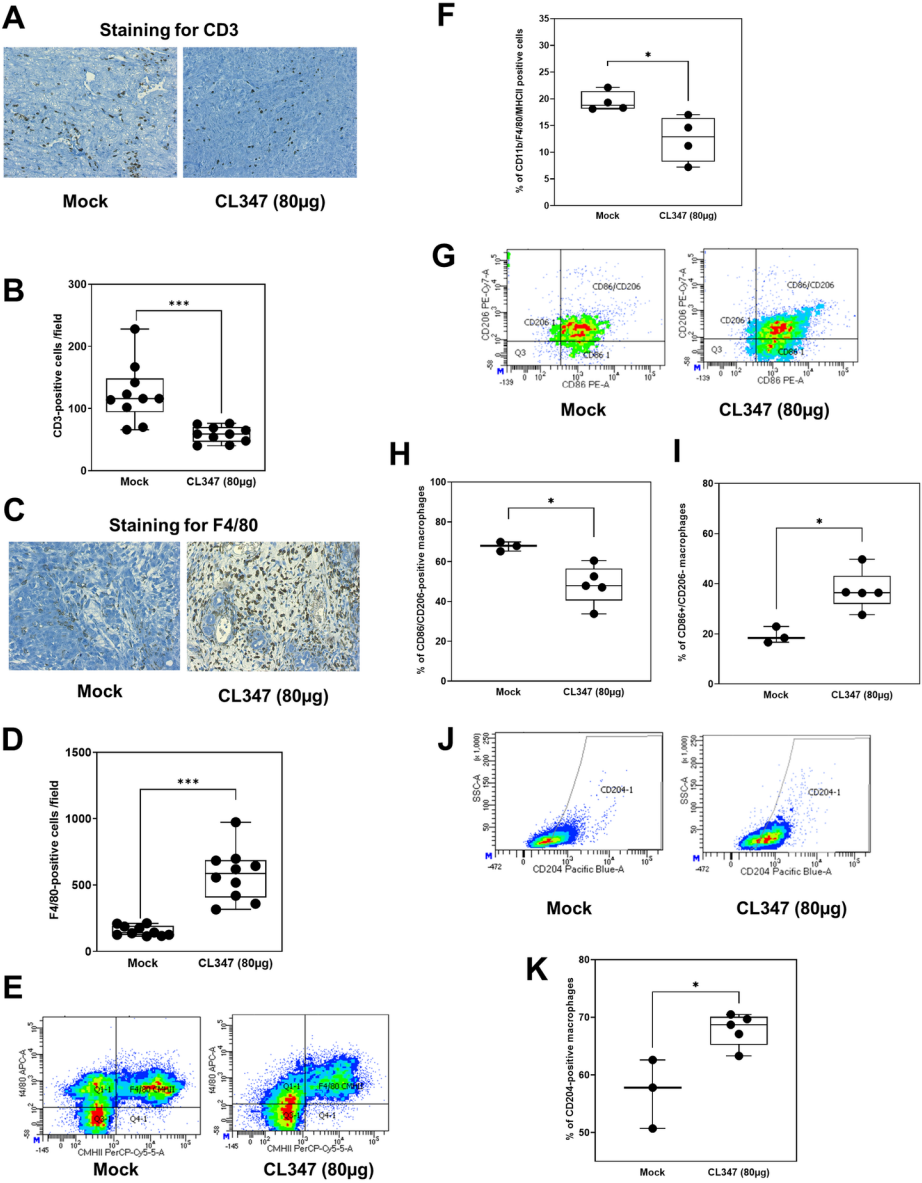
A
Staining for CD3
Mock
CL347 (80μg)
B
CD3-positive cells /field
***
Mock
CL347 (80μg)
C
Staining for F4/80
Mock
CL347 (80μg)
D
F4/80-positive cells /field
***
Mock
CL347 (80μg)
E
F4/80-APC-A
CMHII PerCP-Cy5-5-A
Q1-1
Q4-1
Mock
CL347 (80μg)
F
% of CD11b/F4/80/MHCII positive cells
*
Mock
CL347 (80μg)
G
CD206 PE-Cy7-A
CD86 PE-A
CD86/CD206
CD206-1
CD86-1
Q3
Mock
CL347 (80μg)
H
% of CD86/CD206-positive macrophages
*
Mock
CL347 (80μg)
I
% of CD86+/CD206- macrophages
*
Mock
CL347 (80μg)
J
SSC-A
CD204 Pacific Blue-A
CD204-1
Mock
CL347 (80μg)
K
% of CD204-positive macrophages
*
Mock
CL347 (80μg)

Figure 5

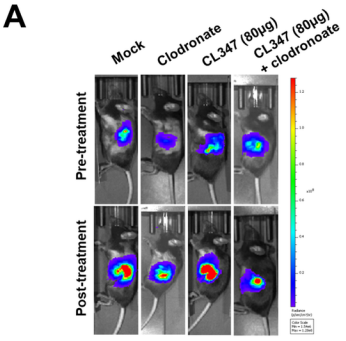
A
Mock
Clodronate
CL347 (80µg)
CL347 (80µg) + clodronoate
Pre-treatment
Post-treatment

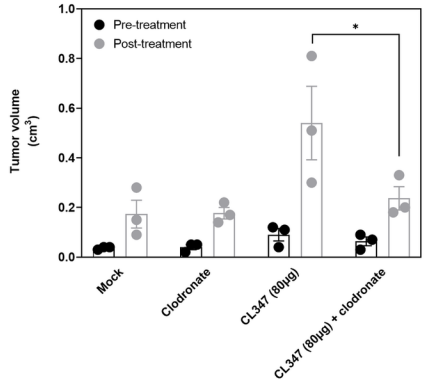
B
Pre-treatment
Post-treatment
Tumor volume (cm3)
1.0
0.8
0.6
0.4
0.2
0.0
*
Mock
Clodronate
CL347 (80µg)
CL347 (80µg) + clodronate

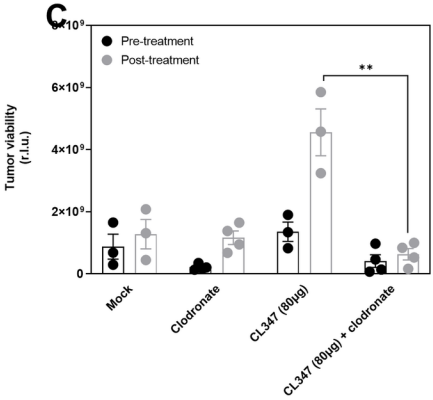
C
Pre-treatment
Post-treatment
Tumor viability (r.l.u.)
8×10⁹
6×10⁹
4×10⁹
2×10⁹
0
**
Mock
Clodronate
CL347 (80µg)
CL347 (80µg) + clodronate

Immune deficient host

TLR7 agonist

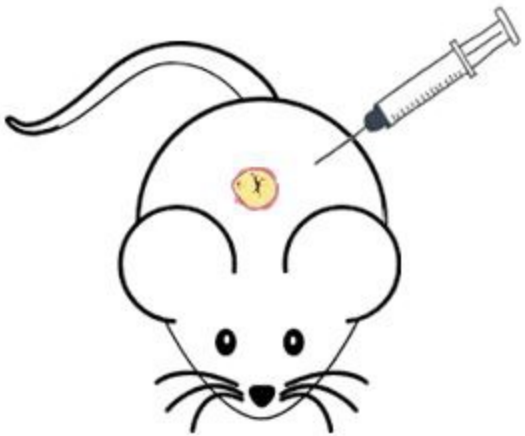

↘ Tumor progression

↗ Mice survival

Immune competent host

TLR7 agonist

Orthotopic experimental pancreatic tumor

↗ Protumoral macrophages

↗ Tumor progression

↘ Mice survival